 한국동력기계공학회지 제11권 제3호 pp.16~21 2007년 8월

Effect of Aspect Ratio on Gas Microchannel Flow
마이크로채널 흐름에 관한 종횡비의 영향

Md. Tajul Islam and Y. W. Lee
타줄 이슬람 · 이연원

Key Words : Knudsen Number (쿠누센 수), Mean Free Path (평균 자유 행로), Rarefaction Effect (희박 효과).

Abstract : Three dimensional numerical study was carried out to investigate the effect of aspect ratio on microchannel flow. We considered five straight rectangular channels with aspect ratios (height/width) 0.2, 0.4, 0.6, 0.8 and 1.0. Nitrogen gas flow was investigated for both slip and noslip wall boundary conditions. Isothermal wall condition was assumed. We used control volume method for this simulation. The slip velocity increases with the increase of aspect ratio. Friction coefficient decreases with the increase of aspect ratio. Slip friction coefficient is lower than noslip friction coefficient. Mass flow rate of slip model is higher than that of noslip model. We compared our results with the experimental result reported in the literature. The agreement was good.

Nomenclature

a	: speed of sound [m/s]
f	: Darcy friction factor
H	: channel height [m]
L	: channel length [m]
Kn	: Knudsen number
u, v, w	: velocity components [m/s]
W	: channel width [m]

Greek symbols

λ_s	: second kind of viscosity
σ_m	: momentum accomodation coefficient
σ_T	: energy accomodation coefficient

Subscripts

AR	: aspect ratio
PR	: pressure ratio
I	: inlet
o	: outlet
1	: reference value

접수일 : 2006년 4월 13일, 채택확정 : 2007년 7월 3일
이연원(책임저자) : 부경대학교 기계공학부
E-mail : ywlee@pknu.ac.kr Tel. 051-620-1417
타줄 이슬람 : 부경대학교 대학원

1. Introduction

The microdevices and microsystems are getting priority day by day. Compactness and high surface to volume ratio are the attractive features of microdevices. The development of micromachining technology enables fabrication of microfluidic devices such as microvalves, micropumps, micronozzles,microsensors, microheat-exchangers etc. Microchannels and chambers are the essential parts of such devices. Microchannles are also used as biochemical reaction chambers, in inkjet print heads, and as heat exchangers for cooling computer chips. It is already established that the flows in microdevices behave differently form those of macro counterparts. The deviation of the state of gas from continuum is measured by the Knudsen number which is defined as $Kn = \frac{\lambda}{L}$, where λ is the mean free path of the molecules and can be calculated using the formula $\lambda = \frac{\mu \sqrt[2]{\pi}}{\sqrt[2]{2p\rho}}$. L is the characteristic length of the channel. A classification of different flow regimes is given as follows.[1]

i) For $Kn \leq 0.01$, the fluid can be considered as continuum. For $Kn \geq 10$, it is considered as free molecular flow.

ii) A rarefied gas with Knudsen number between 0.01 and 10.0 can neither be considered as absolute continuum flow nor free molecular flow. In that region the flow is further classified into slip flow for $0.01 < Kn < 0.1$ and transition flow for $0.1 < Kn < 10$.

Gaseous flow studies in the slip flow regime with continuum hypothesis are not valid but Navier-Stokes equation can be applied to that region with some modifications of boundary conditions on the walls.

Wu and Little[2] performed experiments for both laminar and turbulent gas flow in microchannels. They observed that the measured friction coefficients (fRe) were (10-30%) larger than those predicted by the conventional theory. Choi et. al.[3] measured the friction coefficients for a fully developed laminar flow using glass microtubes having diameters of 3, 7, 10, 53 and 81μm with Reynolds numbers ranging from 30 to 20000. The tubes were very smooth with relative roughness of 0.0003. They found that the Poiseuille number was lower than the conventional value of 64. Yu et. al.[4] conducted experiments through microtubes in silica having diameters of 19, 52 and 102μm for Reynolds numbers ranging from 250 to 20000. They reported that the friction coefficient was lower than that measured by the conventional flow system.

Harley et. al.[5] studied gas flow in silicon microchannels having trapezoidal and rectangular cross sections of hydraulic diameters ranging from 1.01 to 35.91μm. The aspect ratio varied between 0.0053 and 0.161. In this work they observed smaller friction coefficient with respect to the predictions of the conventional theory. Araki el. al.[6] investigated friction coefficients of nitrogen and helium through three different trapezoidal microchannels having hydraulic diameters ranging from 3 to 10μm. The measured friction coefficient was smaller than that predicted by conventional theory. They explained the reduced friction coefficient due to rarefaction effect.

In Pfahler et. al.[7], the flow resistance of nitrogen and helium flows through silicon microchannels having hydraulic diameters ranging from 0.96 to 39.7μm was measured. The observed friction coefficient was smaller than that predicted by the conventional incompressible theory. Arkilic et. al.[8] studied the flow of helium through a rectangular silicon microchannel. They observed lower friction coefficient compared with the conventional result for long channels. Morini and Spiga[9] studied steady, hydrodynamically developed, laminar flow in rectangular duct with first order slip boundary conditions.

Three dimensional studies are rare because of its demand of high computer resources. We used 16 node parallel computer for our investigation. The objective of our investigation is to observe the influence of aspect ratio on gas flow through microchannels for both slip and nolsip wall conditions.

2. Model development

We considered nitrogen gas flow through three dimensional straight rectangular microchannels in Cartesian coordinate system. Figure 1 shows the geometry and coordinate of the microchannel. The channel aspect ratio (height/width) varies from 0.2 to 1.0.

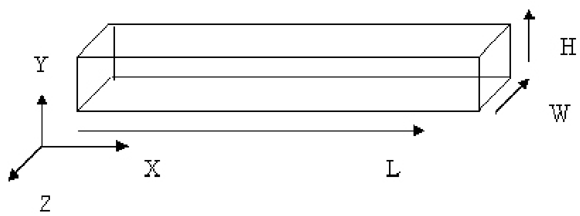

Fig. 1 The geometry of the channel

We considered Maxwell's velocity slip boundary condition and Von Smoluchowski's temperature jump boundary condition on the walls. We assumed the flow to be steady, laminar, and compressible. Gas density was prescribed by the ideal gas law.

Table 1 Physical constants of nitrogen

Parameters	value
Absolute viscosity μ	1.85×10^{-5}(N.s/m^2)
Specific gas constant R	296.7 (J/kg.°K)
Ratio of specific heats γ	1.4

The governing equations are as follows:

Continuity equation

$$\frac{\partial(\rho u)}{\partial x}+\frac{\partial(\rho v)}{\partial y}+\frac{\partial(\rho w)}{\partial z}=0 \tag{1}$$

Momentum equations

$$\rho u\frac{\partial u}{\partial x}+\rho v\frac{\partial u}{\partial y}+\rho w\frac{\partial u}{\partial z}=-\frac{\partial p}{\partial x}+\mu\left[\frac{\partial^2 u}{\partial x^2}+\frac{\partial^2 u}{\partial y^2}+\frac{\partial^2 u}{\partial z^2}+\frac{1}{3}\left(\frac{\partial^2 u}{\partial x^2}+\frac{\partial^2 v}{\partial x\partial y}+\frac{\partial^2 w}{\partial x\partial z}\right)\right] \tag{2}$$

$$\rho u\frac{\partial v}{\partial x}+\rho v\frac{\partial v}{\partial y}+\rho w\frac{\partial v}{\partial z}=-\frac{\partial p}{\partial y}+\mu\left[\frac{\partial^2 v}{\partial x^2}+\frac{\partial^2 v}{\partial y^2}+\frac{\partial^2 v}{\partial z^2}+\frac{1}{3}\left(\frac{\partial^2 u}{\partial x\partial y}+\frac{\partial^2 v}{\partial y^2}+\frac{\partial^2 w}{\partial y\partial z}\right)\right] \tag{3}$$

$$\rho u\frac{\partial w}{\partial x}+\rho v\frac{\partial w}{\partial y}+\rho w\frac{\partial w}{\partial z}=-\frac{\partial p}{\partial z}+\mu\left[\frac{\partial^2 w}{\partial x^2}+\frac{\partial^2 w}{\partial y^2}+\frac{\partial^2 w}{\partial z^2}+\frac{1}{3}\left(\frac{\partial^2 u}{\partial x^2}+\frac{\partial^2 v}{\partial y\partial z}+\frac{\partial^2 w}{\partial z^2}\right)\right] \tag{4}$$

Energy equation

$$\begin{aligned}\rho c_p\left(u\frac{\partial T}{\partial x}+v\frac{\partial T}{\partial y}+w\frac{\partial T}{\partial z}\right)&=\left(u\frac{\partial p}{\partial x}+v\frac{\partial p}{\partial y}+w\frac{\partial p}{\partial z}\right)\\&+k\left(\frac{\partial^2 T}{\partial x^2}+\frac{\partial^2 T}{\partial y^2}+\frac{\partial^2 T}{\partial z^2}\right)+\\&\mu\left(2\left(\frac{\partial u}{\partial x}\right)^2+2\left(\frac{\partial v}{\partial y}\right)^2+2\left(\frac{\partial w}{\partial z}\right)^2\right)\\&+\mu\left(\frac{\partial u}{\partial y}+\frac{\partial v}{\partial x}\right)^2+\mu\left(\frac{\partial w}{\partial y}+\frac{\partial v}{\partial z}\right)^2+\mu\left(\frac{\partial w}{\partial x}+\frac{\partial u}{\partial z}\right)^2\\&-\frac{2\mu}{3}\left(\frac{\partial u}{\partial x}+\frac{\partial v}{\partial y}+\frac{\partial w}{\partial z}\right)\end{aligned} \tag{5}$$

The equation of state for ideal gas

$$p=\rho RT \tag{6}$$

We used Stoke's hypothesis[11] $\lambda_s+\frac{2}{3}\mu=0$, in momentum and energy equations.

We normalized the variables as follows:

Velocities (u, v, w) were normalized by the characteristic inlet sound velocity a_1. Sound velocity is defined by $a=\sqrt[2]{\gamma RT}$. Mean free path λ was normalized by channel height H. Temperature T and density ρ were normalized by the reference temperature T_1 and reference density ρ_1 respectively. Pressure p was normalized by $\rho_1 a_1^2$. Cross sectional Reynolds number is defined by $Re=\frac{\bar{\rho}\bar{u}Dh}{\mu}$, where $\bar{\rho}$ is the cross sectional average density. The hydraulic diameter was defined by $Dh=\frac{2^*W^*H}{(W+H)}$.

3. Boundary conditions

3.1 Slip wall boundary conditions

We assumed the flow steady state and isothermal. The slip velocity boundary condition was proposed by Maxwell for an isothermal flow:[10]

$$u_{gas}-u_{wall}=\frac{2-\sigma_m}{\sigma_m}Kn\frac{\partial u_s}{\partial n} \tag{7}$$

and the temperature jump boundary conditions by Von Smoluchowski as

$$T_{gas}-T_{wall}=\frac{2-\sigma_T}{\sigma_T}\left(\frac{2\gamma}{\gamma+1}\right)\frac{Kn}{\mathrm{Pr}}\frac{\partial T}{\partial n} \tag{8}$$

where $\frac{\partial u_s}{\partial n}$ and $\frac{\partial T}{\partial n}$ show the variation of tangential velocity and temperature normal to the wall. The slip conditions expressed in (7) and (8) are in normalized form. The coefficients σ_m and σ_T are the tangential momentum and energy accommodation coefficients respectively. In the present study we considered σ_m=1 and σ_T=1.

3.2 Numerical Method

The governing equations were solved by control volume method. Continuity and momentum equations were solved with the second order upwind implicit scheme. SIMPLE algorithm was used for pressure-velocity coupling. The energy equation was also solved by second order upwind scheme. The domain was divided in to small volume of hexahedral cells. The maximum number of cells we used for the largest domain was 3.6 million. Convergence criterion was set as normalized residual to 10^{-8} for energy equation and 10^{-6} for all other equations.

3.3 Grid independency test

To evaluate the grid size effect grid independency test were carried out. Three different sizes of grid $8\times30\times1801$, $10\times46\times1801$ and $10\times46\times3001$ were tested for the channel with aspect ratio 0.2. The difference in velocities of the first two sizes of grid was 4.31%. The velocities of the last two sizes of grid are almost the same. The difference of velocity is only 1.2%. we selected the grid size $10\times46\times1801$ for our simulation.

4. Result and discussion

To validate our simulation we first simulated compressible nitrogen flow in a square conventional channel with hydraulic diameter 1cm. We used the pressure ratio (inlet/outlet) 1.0001. The outlet was atmospheric pressure condition. The wall and gas temperature was fixed to 310° K. As the pressure ratio was small the flow was very close to incompressible flow. We computed friction coefficient (fRe).

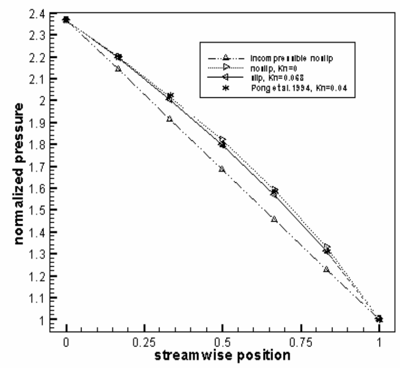

Fig. 2 Comparison of pressure distribution with the experimental result

In our simulation it was 56.20 which was very close to the theoretical value of 56.91. To validate our result further we simulated nitrogen gas flow in a microchannel of dimensions 1.2μm height, 40 μm width and 3000μm long. We used Pressure ratio 2.36. We compared the result with the reported experimental result[11]. The dotted straight line expresses the pressure distribution of incompressible flow which is linear. Compressible flow shows nonlinear pressure distribution. Flow with Kn=0 shows the highest Nonlinearity. In present simulation Knudsen number was 0.068 which is very close to the knudsen number (0.04) used by Pong et. al. The pressure distribution shows good agreement with the pressure distribution by Pong et. al.

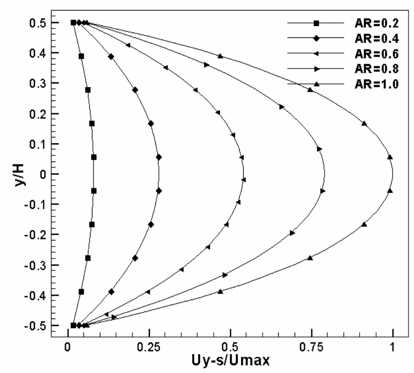

Fig. 3 Slip velocity distribution

Figure 3 shows the normalized cross sectional slip velocity distribution near outlet for different aspect ratios. Velocity distribution shows that the velocity increases with the increase of aspect ratio.

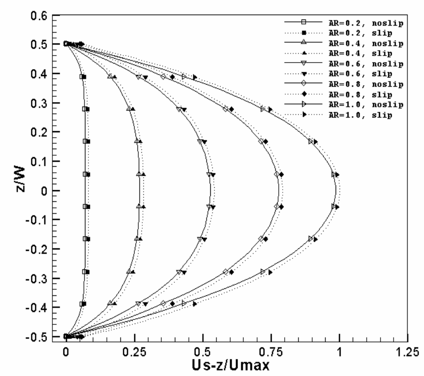

Fig. 4 Slip and noslip velocity distribution

Figure 4 depicted the slip and noslip velocity distribution for different aspect ratios. It is evident that the slip velocity is higher than the noslip velocity. Velocity for both the cases increases towards the streamwise direction and is maximum at the outlet. Figure 5 shows the crosswise centerline slip velocity. Uz-s indicates the velocity on the plane that crosses the side walls horizontally and passes through the line y=0. Uy-s indicates the velocity on the plane that crosses the top and bottom walls vertically and passes through the line z=0. It is clear from the figure that the slip velocity on the walls are different. For a particular case of aspect ratio 0.2, Uy-s velocity on the wall is higher than that of Uz-s.

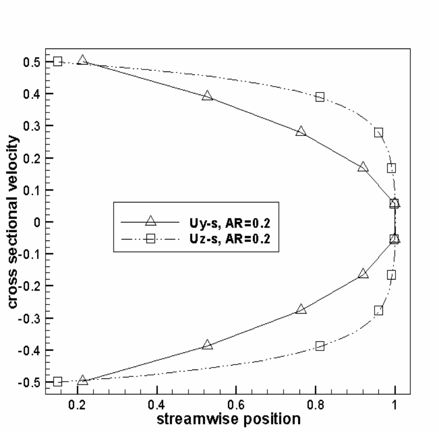

Fig. 5 slip velocity distribution across the opposite walls for AR=0.2

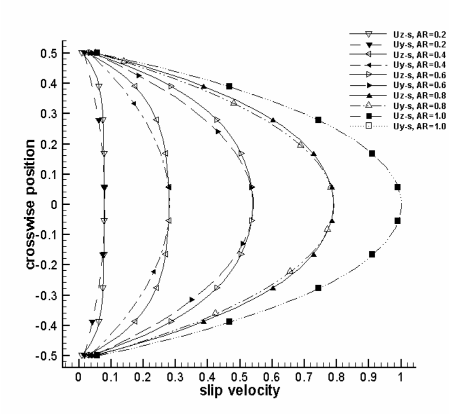

Fig. 6 slip velocity distribution across the opposite walls for different AR

In Fig. 6, Uz-s and Uy-s are shown for different aspect ratios. When the aspect ratio is 1 then Uz-s and Uy-s are equal and the velocity distributions are the same. As the aspect ratio decreases, the difference of Uz-s and Uy-s increases.

Figure 7 shows the comparison of mass flow rate of slip and noslip model for different hydraulic diameters.The mass flow rate for slip model is higher than noslip model which is consistent with the result that the velocity of slip model is higher than that of noslip model. The influence of hydraulic diameter on mass flow rate is significant.

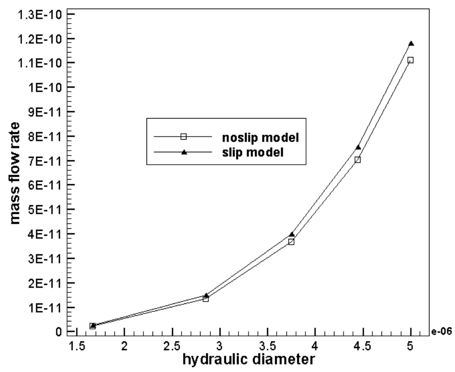

Fig. 7 Mass flow rate for different hydraulic diameters

For both slip and noslip model mass flow rate and their difference increases with the increase of hydraulic diameter.

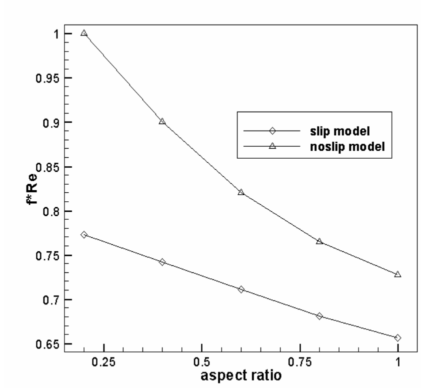

Fig. 8 friction constant as a function of aspect ratio

Figure 8 depicted the variation of friction coefficient as a function of aspect ratio. Channel aspect ratio has a significant influence on friction coefficient. Friction coefficient decreases with the increase of aspect ratios.

In our simulation for noslip compressible flow in square channel friction coefficient is 57.72. This value increases with decreasing aspect ratio and ranges from 57.72 to 79.36 for the change of aspect ratio from 1 to 0.2. For slip flow the value of fRe for square microchannel is 52.08. This value ranges from 52.08 to 61.30 for the variation of aspect ratio from 1 to 0.2.

5. Conclusion

Three dimensional numerical study was carried out to observe the influence of aspect ratio on gas flow through microchannels for both slip and nolsip wall conditions. The investigation results can be summarized as follows:

1) The slip velocity increases with the increase of aspect ratios.
2) For slip boundary condition the friction coefficient for square microchannel is much lower than the conventional value.
3) The friction coefficient for slip model is lower than that of noslip model.
4) The cross sectional velocities on the opposite walls denoted by Uy-s and Uz-s are different for lower aspect ratio.

Acknowledgement

This work was supported by the Korean Research Foundation Grant Funded by the Korean Government (MOEHRD), (KRF-2004-2-48).

Reference

1) S. A. Schaaff and P. L. Chambre, 1961, "Flow of Rarefied gases", Princeton University Press, Princeton, NJ.
2) P. Wu and W. A. Little, 1983, "Measurement of friction factors for the flow of gases in very fine channels used for microminiature Joule-Thomson refrigerators", Cryogenics, Vol. 23, No. 5, pp. 273～277.
3) S. B. Choi, R. F. Barron and R. O. Warrington, 1991, "Fluid flow and heat transfer in microtubes", in: Micromechanical sensors, Actuators and Systems, ASME DSC Atlanta, Vol. 32, pp. 123～134.
4) D. Yu, R. O. Warrington, R. Barron and T. Ameel, 1995, "An experimental and theoretical investigation of fluid flow and heat transfer in microtubes", Preceedings of ASME/JSME Thermal Enginering joint conference, Maui, HI, pp. 523～530.
5) John C. Harley, Yufeng Huang, Haim H. Bau and J. N. Zemel, 1995, "Gas flow in microchannels", J. Fluid Mech., Vol. 284, pp. 257～274.
6) Takuto Araki, Min Soo Kim, Hiroshi Iwai, and Kenjiro Suzuki, 2002, "An experimental investigation of gaseous flow characteristics in microchannels", Thermophysical Engineering, Vol. 6, pp. 117～130.
7) J. Pfahler, Yufeng Huang, Haim H. Bau and J. N. Zemel, 1991, "Gas and Liquid Flow in Small Channels", Micromechanical Sensors, Actuators and Systems, ASME, New York, DSC-Vol. 32, pp. 49～60.
8) Errol B. Arkilic, Kenneth S. Breuer and Martin A. Schmidt, 1994, "Gaseous flow in microchannels", Application of Microfabrication to Fluid Mechanics, ASME FED-Vol. 197, pp. 57～66.
9) G. L. Morini and M. Spiga, 1998, "Slip flow in rectangular microtubes", Microscale Thermophysical. Eng., Vol. 2, pp. 273～282.
10) M. Gad-el-Hak (Ed.), 2001, "The MEMS Handbook", CRC press, New York.
11) Pong, K. -C.; Ho, C. -M.; Liu, J. and Tai, Y. C., 1994, "Non-linear pressure distributioin in uniform microchannels", Application of Microfabrication of Fluid Mechanics, ASME FED-Vol. 197, pp. 51～56.